Inorganic Chemistry

ARTICLE

pubs.acs.org/IC

Solvent Induced Diverse Dimensional Coordination Assemblies of Cupric Benzotriazole-5-carboxylate: Syntheses, Crystal Structures, and Magnetic Properties

Juan Xiao, Bao-Yu Liu, Gang Wei, and Xiao-Chun Huang*

Department of Chemistry, Shantou University, Shantou, Guangdong Province, 515063 China

Supporting Information

ABSTRACT: Three cupric coordination assemblies $[Cu(btca)(H_2O)_2]$ (**1**), $[Cu(btca)(H_2O)_{3.5}]_8 \cdot 16H_2O$ (**2**), and $[Cu_{2.5}(btca)_{1.5}(Hbtca)_{0.5}(\mu\text{-}Cl)_{0.5}(\mu_3\text{—}OH)(H_2O)] \cdot H_2O$ (**3**) have been solvothermally synthesized by cupric salts and a bifunctional ligand benzotriazole-5-carboxylic acid (H_2btca) in different solvent medium. These complexes were structurally characterized by X-ray diffraction analyses and further identified by infrared spectra (IR), elemental analyses, powder X-ray diffraction (PXRD), and thermogravimetric analyses (TGA). Single crystal structural analysis shows that these coordination compounds assembled by the almost same reactants present diverse dimensional crystal structures, wherein **1** possesses two-dimensional (2D) layers with (4.8^2) topology, the zero-dimensional (0D) neutral metallomacrocycle with flat octagonal geometry in **2** connects each other through hydrogen bonding to extend to be a three-dimensional (3D) nanotubular network, and **3** exhibits 3D framework with 1D honeycomb channels constructed by the strip-shaped chains containing $[Cu_5(\mu_3\text{-}OH)_2(btca)_4]^-$ pentaclusters bridging to the adjacent $Cu_6(btca)_{12}^{6-}$ cages. The diversity of these structures mainly stems from the versatile coordination modes of the anionic ligand in each compound, especially the 1,2,3-triazolate group: bidentate $\mu_{1,2}$ bridging mode in **1**, bidentate $\mu_{1,3}$ bridging mode in **2**, and tridentate $\mu_{1,2,3}$ bridging mode in **3**, respectively. Furthermore, the magnetic properties of **1**—**3** have been investigated as well.

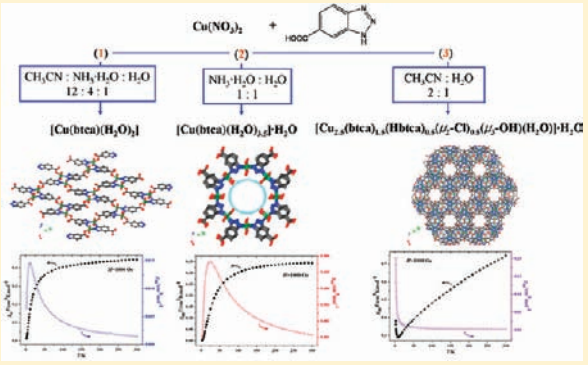

INTRODUCTION

Over the past decade, coordination polymers (CPs) have emerged as one of the most promising classes of microporous materials, particularly in view of their potential applications.[1] A large number of cagelike and macrocyclic structures have been obtained via rationally designed metal directional self-assembly approach, which has attracted a great deal of attention in recent years not only because of their structure diversity such as molecular polygons,[2] bowls and cages, nanotubes, and so on, but also due to the rich physical properties of the metal-assembled systems in magnetism, luminescence, and the exciting applications in selective guest inclusion, drug delivery, molecular recognition, catalysis, and biological mimicry.[3] Thus, rational selection of metal centers and organic ligands with suitable shape, functionality, flexibility, and symmetry makes a pivotal role in synthesizing CPs with desired structures and properties. Meanwhile, solvents often affect the coordination behavior of the metal ions, which may determine the connectivity and dimensionality of the overall network. Guest solvent molecules can also affect the thermal stabilities via intermolecular interactions with the parent frameworks. Therefore, systematic investigation of an assembling system with the fixed metal centers and coordination organic molecules is crucial for gaining expected target product.

Up to now, multidentate N-donor[4] or O-donor[5] ligands have been employed extensively in the construction of extended structures. Among various ligands, imidazolate, triazolate, polycarboxylates, and their derivatives have attracted much more attention for constructing a series of metal—organic materials.[6] Much effort has also been focused on syntheses of novel functional materials based on the aromatic organic ligands containing carboxylic and nitrogen donor groups, such as imidazole-4,5-dicarboxylic acid (H_3IDC),[7] 1,2,3-triazole-4,5-dicarboxylic acid (H_3tzdc),[8] 1-*H*-benzimidazole-5-carboxylic acid (H_2bic),[9] and benzimidazole-5,6-dicarboxylic acid (Hbidc).[10] These multifunctional ligands easily coordinate with metal ions to form multidimensional complexes. Nevertheless, controlling the dimension and obtaining the particular target product remain poorly reported because of the challenging difficulty of their preparation approach.[11] Furthermore, coordination compounds with backbones constructed from N-donor ligands and O-donor ligands together to enhance the dimensionality and enrich the versatility of coordination polymers have been successfully reported.[12] However, for constructing a target network one needs

Received: July 22, 2011
Published: October 07, 2011

dx.doi.org/10.1021/ic201571n | *Inorg. Chem.* 2011, 50, 11032–11038

Scheme 1. Syntheses of Complexes 1−3

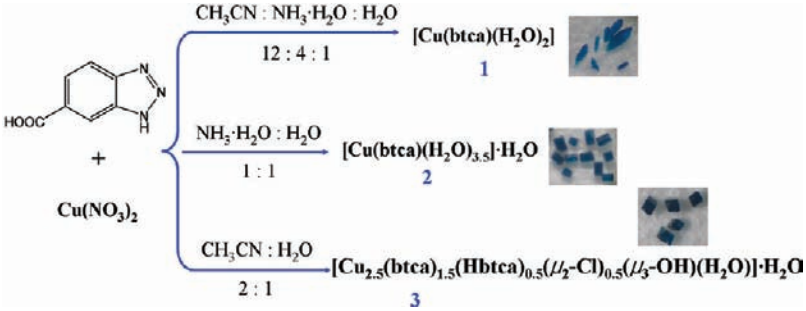

to overcome uncertain factors which arise from the versatile linkers and variable coordination geometry of metal ions.

Herein, we choose a polydentate ligand, benzotriazole-5-carboxylate acid (H_2btca), as organic linker based on the following considerations: (i) the special orientation between 1,2,3-triazole and carboxyl groups may obtain intriguing metal−organic frameworks (MOFs) with exceptional discrete fragments as secondary building units (SBUs); (ii) the strong π-conjugate system from large benzotriazole ring can strengthen the stability of the structures; (iii) five coordination atoms can potentially act as hydrogen bond acceptors and donors to assemble supramolecular structures. To the best of our knowledge, the development of novel coordination networks based on this ligand is still in its infancy.[13] In this work, we systematically investigated the assembling reactions of cupric salts with this ligand, and three intriguing complexes, namely $[Cu(btca)(H_2O)_2]$ (**1**), $[Cu(btca)(H_2O)_{3.5}]_8\cdot 16H_2O$ (**2**), and $[Cu_{2.5}(btca)_{1.5}(Hbtca)_{0.5}(\mu\text{-Cl})_{0.5}(\mu_3\text{−OH})(H_2O)]\cdot H_2O$ (**3**), are obtained (Scheme 1). Interestingly, their structures display diversities in which **1** shows a two-dimensional (2D) network, **2** presents a neutral planar metallomacrocyclic structure, and **3** behaves as a 3D porous honeycomb-like structure. The magnetic properties of these three coordination compounds have also been characterized.

EXPERIMENTAL SECTION

Materials and Methods. $Cu(NO_3)_2\cdot 3H_2O$, benzotriazole-5-carboxylic acid (H_2btca), acetonitrile (MeCN), and ammonia−water ($NH_3\cdot H_2O$) were obtained from commercial sources and were used as received without further purification. The phase-purity of each product was checked by powder X-ray diffraction (PXRD) using a Rigaku D/M-2200T automated diffractometer. Infrared spectra were recorded on a Nicolet Avatar 360 FTIR spectrophotometer as KBr pellets in the 400−4000 cm^{-1} region. Elemental analyses (C, H, N) were performed with a Vario EL elemental analyzer. Thermogravimetric analyses (TGA) were performed by heating the crystalline sample from 30 to 800 °C at a rate of 10 °C min^{-1} under nitrogen gas flow on Netzsch STA 449C equipment.

Synthesis of $[Cu(btca)(H_2O)_2]$ (1). A mixture of $Cu(NO_3)_2\cdot 3H_2O$ (0.0243 g, 0.1 mmol), H_2btca (0.0164 g, 0.1 mmol), MeCN (6.0 mL), $NH_3\cdot H_2O$ (2.0 mL), and H_2O (0.5 mL) was put into a 15-mL Teflon-lined stainless autoclave and heated to 140 °C for three days (volume ratio of $MeCN/NH_3\cdot H_2O/H_2O \approx 12{:}4{:}1$). This was then slowly cooled to room temperature. Blue platelet crystals of **1** were obtained in about 60% yield (0.0156 g) based on H_2btca. Elemental Anal. (%) for $C_7H_7N_3O_4Cu$ Calcd: C, 32.25; H, 2.71; N, 16.12. Found: C, 32.21; H, 2.76; N, 16.07. IR (KBr, cm^{-1}): 3449 (w), 3355 (m), 3309 (s), 3213 (s), 1644 (m), 1582 (s), 1548 (s), 1475 (w), 1383 (s), 1271 (m), 1235 (s), 1185 (m), 1153 (m), 897 (w), 793 (m), 757 (m), 692 (m), 603 (w), 559 (w), 406 (w).

Synthesis of $[Cu(btca)(H_2O)_{3.5}]_8\cdot 16H_2O$ (2). A mixture of $Cu(NO_3)_2\cdot 3H_2O$ (0.1 mmol, 0.0243 g), H_2btca (0.1 mmol, 0.0164 g), $NH_3\cdot H_2O$ (2.0 mL), and H_2O (2.0 mL) was put into a 15-mL Teflon-lined stainless autoclave and heated to 140 °C for three days (volume ratio of $NH_3\cdot H_2O/H_2O \approx 1{:}1$). This was then slowly cooled to room temperature. Blue columnar crystals of **2** were obtained in about 40% yield (0.0130 g) based on H_2btca. Elemental Anal. for $C_{56}H_{112}N_{24}O_{60}Cu_8$ Calcd: C, 25.97; H, 4.36; N, 12.98. Found: C, 26.07; H, 4.30; N, 12.90. IR (KBr, cm^{-1}): 3173 (s), 1620 (m), 1588 (s), 1541 (s), 1384 (s), 1286 (m), 1172 (w), 795 (m), 710 (w), 591(w), 540 (w).

Synthesis of $[Cu_{2.5}(btca)_{1.5}(Hbtca)_{0.5}(\mu\text{-Cl})_{0.5}(\mu_3\text{−OH})(H_2O)]\cdot H_2O$ (3). A mixture of $Cu(NO_3)_2\cdot 3H_2O$ (0.3 mmol, 0.0730 g), H_2btca (0.2 mmol, 0.0330 g), NaCl (0.05 mmol, 0.003 g), MeCN (4.0 mL), and H_2O (2.0 mL) was put into a 15-mL Teflon-lined stainless autoclave and heated to 140 °C for three days (volume ratio of $MeCN/H_2O \approx 2{:}1$). This was then slowly cooled to room temperature. Glaucous block crystals of **3** were obtained in about 55% yield (0.0304 g) based on H_2btca. Elemental Anal. for $C_{14}H_{11.5}N_6O_7Cl_{0.5}Cu_{2.5}$ Calcd: C, 30.44; H, 2.10; N, 15.21. Found: C, 30.40; H, 2.22; N, 15.17. IR (KBr, cm^{-1}): 3368 (s), 1593 (s), 1548 (s), 1379 (s), 1299 (w), 1220 (m), 1162 (w), 1101 (w), 1055 (w), 810 (m), 781(m), 755 (m), 610 (w).

X-ray Crystallography. All single crystals of these three complexes were carefully selected under an optical microscope and glued to thin glass fibers. Structural measurements were performed on a computer-controlled Siemens Smart CCD diffractometer with graphite-monochromated Mo Kα radiation (λ = 0.710 73 Å) at 295 K. Absorption corrections were applied by using the multiscan program SADABS. Structural solutions and full-matrix least-squares refinements based on F^2 were performed with the SHELX-97 program packages, respectively. Anisotropic thermal parameters were applied to all non-hydrogen atoms. All the hydrogen atoms were generated geometrically. Crystal data as well as details of data collection and refinements for the complexes are summarized in Table S1. Atomic positional parameters, full tables of bond lengths and angles, and anisotropic temperature factors are available in the Supporting Information. Selected bond lengths and bond angles are given in Table S2.

RESULTS AND DISCUSSION

Syntheses and Characterization. These complexes in this work were prepared in modest to good yields by exploiting the hydrothermal reactions on the basis of selection of reaction solvents, while the other synthetic parameters were intentionally held constant. The same initial reactants in different solvent medium can tune the structural diversities of coordination assemblies. Compound **1** was synthesized by using a mixture of

three solvents (acetonitrile/ammonia−water/deionized water ≈ 12:4:1), while **2** was obtained without acetonitrile in the reaction system (ammonia−water/deionized water ≈ 1:1), and **3** was prepared during the reaction medium of acetonitrile and water (ca. 2:1) in the presence of chloride. The synthesis of **2** indicates that the ammonia−water as basic medium plays an important role in the formation of the final metallomacrocyclic structure, and water molecules can be used to coordinate to central copper(II) ions to prevent its further extension and act as hydrogen bonding linkers to form supramolecular architecture simultaneously. In addition, the different products of **1**, **2**, and **3** mainly result from the different mixed solvents used in the reactants. X-ray quality crystals of **3** could only be obtained when sodium chloride was used. To explore the phenomenon, experiments using other cupric salts instead of $Cu(NO_3)_2$ were performed in the absence of chloride ions, and then the PXRDs of these products were determined, which are identical to the PXRD pattern of **3** (Figure S4), indicating that the anions in the Cu(II) salts are not the crucial factor for the formation of this framework in **3**. The charge-balancing chloride ions in **3** could be replaced by other anions such as hydroxide ions in the reaction system without chloride ions, which can also act as μ_2-bridging ligands the same as chloride in **3** to coordinate to copper ions.

All samples were filtered, washed with ethanol, and dried in air. The samples used for all property determination were single crystals and selected using a microscope. Phase purities of the measured samples were confirmed by PXRD patterns (patterns for all of complexes can be found in Figures S3−5). IR spectra of **1**−**3** show characteristic bands of 1500−1650 cm^{-1} and 1380−1400 cm^{-1} (C═O, C═N stretching of btca ligand) and a strong broad band at 3100−3400 cm^{-1} which could be attributed to ν(O−H) of the water molecules.

Structure Description. As a result of single-crystal X-ray diffraction analyses, it is shown that one has a 2D network $[Cu(btca)(H_2O)_2]$ (**1**), and $[Cu(btca)(H_2O)_{3.5}]_8 \cdot 16H_2O$ (**2**) possesses a nanoporous hydrogen-bonded nanotubular structure, while the third exhibits 3D porous framework $[Cu_{2.5}(btca)_{1.5}(Hbtca)_{0.5}(\mu\text{-Cl})_{0.5}(\mu_3\text{-OH})(H_2O)] \cdot H_2O$ (**3**).

The 2D layer (**1**) is composed of distorted square pyramidal coordinated Cu(II) centers, which is coordinated by two nitrogen atoms (N2, N3) and one oxygen atom (O1) from three different btca ligands, and two water molecules occupied the remaining coordination sites (Figure 1a). However, the presence of two terminal water molecules precludes the two-dimensional layer from being extended to a higher dimensional network (Figure 1b). Meanwhile, the packing diagram shows that a 3D network is formed through offset face to face stack interactions of benzotriazolate rings between adjacent layers (the dihedral angle between the paralleling rings being ca. 4.9° with the distance of 3.829(5) Å). In addition, the hydrogen bonding interactions (O2···O4 2.974(4) Å; O2···O3 3.401(5) Å) involving the coordinated water supply the additional stability effect for the 3D structure (Figure 1c), which could be simplified to be a 3-connected 4.8^2 net while regarding btca ligands as 3-connected nodes and Cu(II) ions as linkers (Figure 1d).

In **2**, Cu1 with the square pyramidal coordination geometry is formed by two nitrogen atoms of btca ligand at its axial positions and three oxygen atoms from water at the equatorial positions, and Cu2 is coordinated one more oxygen atoms from water at the equatorial positions than Cu1 to give a distorted octahedral coordination sphere (Figure 2a). The main and basic unit in **2** is

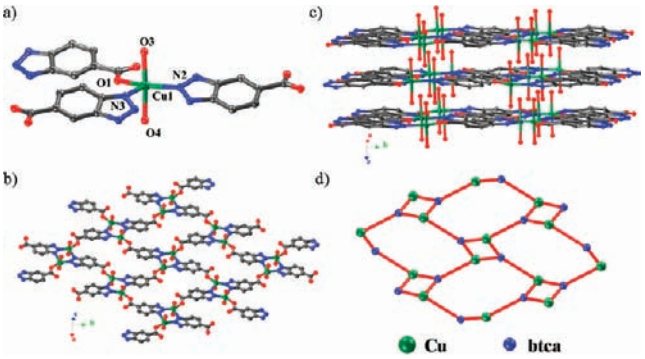

Figure 1. (a) Coordination environment of Cu^{2+} ion in **1**. (b) View of the 2D structure in **1**. (c) 3D structure of **1** via $\pi\cdots\pi$ and hydrogen bonding interactions. (d) 3-connected 4.8^2 net in **1**.

$[Cu(btca)]_8$ rings constructed by eight btca ligands and eight copper(II) ions (Figure 2b). All btca ligands in one ring are locked in a coplanar geometry, and adopt an imidazolate bridging type to coordinate to copper(II) ions. The most interesting feature of the structure of **2** is the arrangement of the octagons into hydrogen bonding nanotubes. The 1-D channels can be observed running parallel along the *c*-axis in **2** (Figure 2d), and have a size of around 10.346(8) Å in interior tubular diameter. The three-dimensional framework (Figure 2e) is built via hydrogen bonding interactions of oxygen atoms from btca ligand and a coordinated water molecule (O2···O3 2.848(5) Å), anchored by benzene rings between adjacent $[Cu(btca)]_8$ cyclic units (the distance between them being 3.721(3) Å, Figure 2c). The lattice water molecules (not shown) are embedded in the tubes involved in intermolecular hydrogen bonding. The disordered lattice water molecules occupy approximately 27.0% of the framework voids with a volume of about 1563.0 $Å^3$ in each cell unit estimated by using PLATON software.

The ring structures by use of metal ions and ligands are common,[14] but the similar examples using metal ions and ligands at 1:1 molar ratio are rare.[15] However, steric hindrance and other factors from ligands can lead to ring distortion and/or dislocation and reduce the passageway diameter. Furthermore, only limited examples of planar metallomacrocycles species have been reported. In this work, hydrogen bonding interactions between cyclic units and strong conjugation from the ligand result in the formation of a 3D nanoporous hydrogen-bonded metal−organic framework with octagonal metallomacrocycles. It appears likely that this strategy could be used to lock the geometries of even larger rings, by using readily available ligands.

The asymmetric unit of **3** consists of three unique Cu(II) ions as shown in Figure S1. Cu1 adopts a distorted square pyramidal coordination geometry that is formed by three nitrogen atoms from three symmetry-related btca ligands, one hydroxide, and one chloride. Cu2 has distorted octahedral coordination geometry and is ligated by one hydroxide, two nitrogen atoms, and three oxygen atom from btca ligands. The Cu3 ion locates at the special position and adopts the octahedral coordination geometry with two hydroxides, two nitrogen atoms from two btca ligands, and two coordinated water molecules.

In particular, two triangular clusters $[Cu_3(\mu_3\text{-OH})]^{4+}$ are linked together by sharing Cu3 to form $[Cu_5(\mu_3\text{-OH})_2(btca)_4]^-$ pentaclusters, which are linked by Cu1 to give a strip-shaped chain along the *b* axis direction (Figure 3a). In the meantime, the $Cu_6(btca)_{12}^{6-}$ cages are formed by use of Cu2 and btca ligands

dx.doi.org/10.1021/ic201571n |*Inorg. Chem.* 2011, 50, 11032–11038

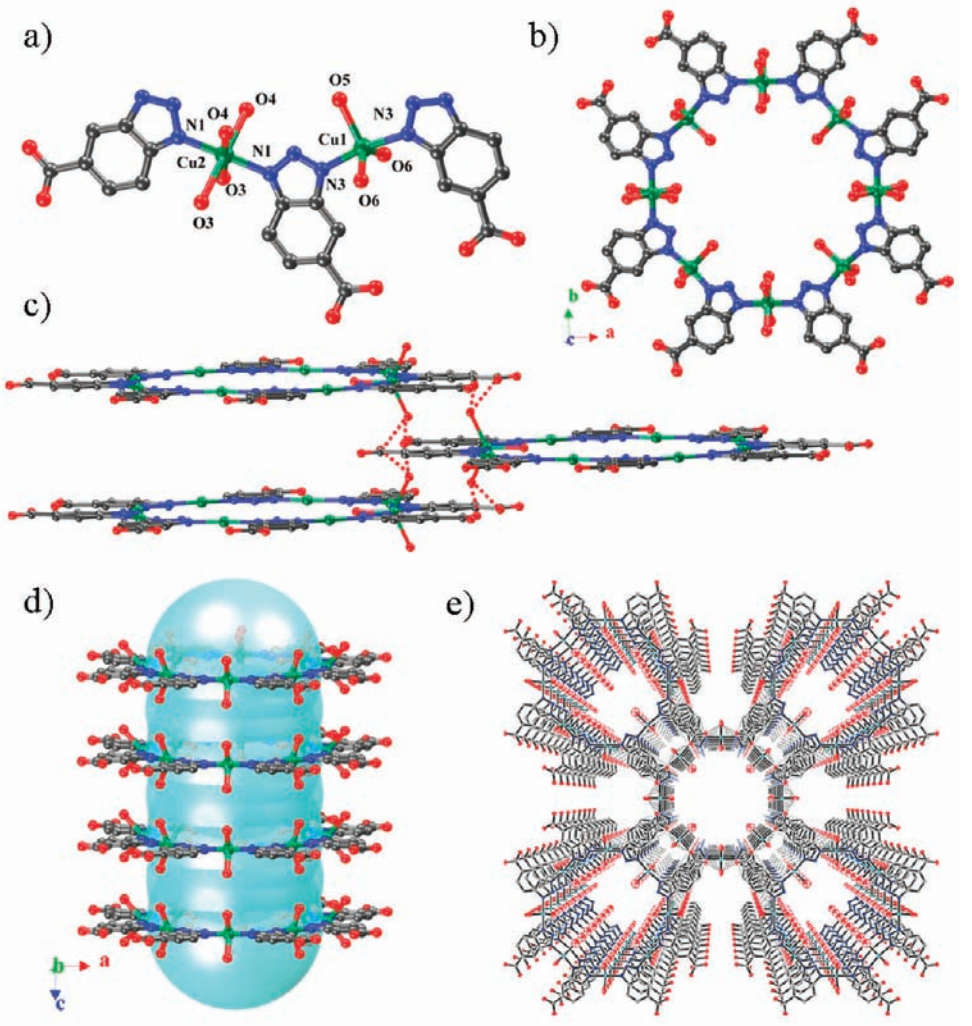

Figure 2. (a) Coordination environment of two Cu^{2+} ions in **2**. (b) $[Cu(btca)]_8$ ring unit. (c) Hydrogen bonded interactions between octagon rings in **2** (O atoms from coordinated water molecules omitted for clarity). (d) 1D channel formed by paralleling stacking of octagon rings along the *c* axis in **2**. (e) Packing diagram of **2**.

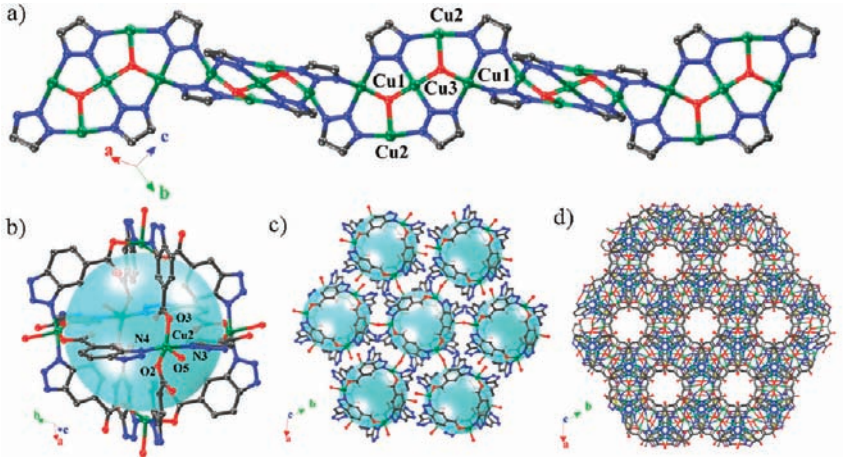

Figure 3. (a) Metal hydroxide strip-shaped chain (for clarity the btca ligands are truncated) of **3**. (b, c) $Cu_6(btca)_{12}^{6-}$ cage and stacked diagram composed by the cage units in **3**. (d) 3D framework of **3**.

(Figure 3b,c). Each strip-shaped chain is connected with four identical chains via the btca oxygen atoms to generate a 3D metal−organic framework encompassing a considerable solvent-accessible volume with 1D hexagonal channels (Figure 3d),

dx.doi.org/10.1021/ic201571n |*Inorg. Chem.* 2011, 50, 11032–11038

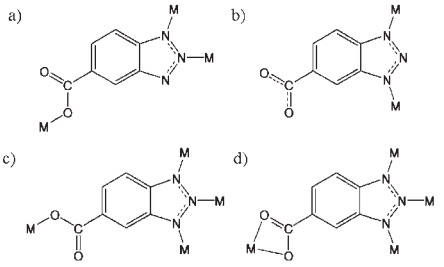

Figure 4. Bridging fashion of btca ligand observed in this work (a for **1**, b for **2**, c and d for **3**).

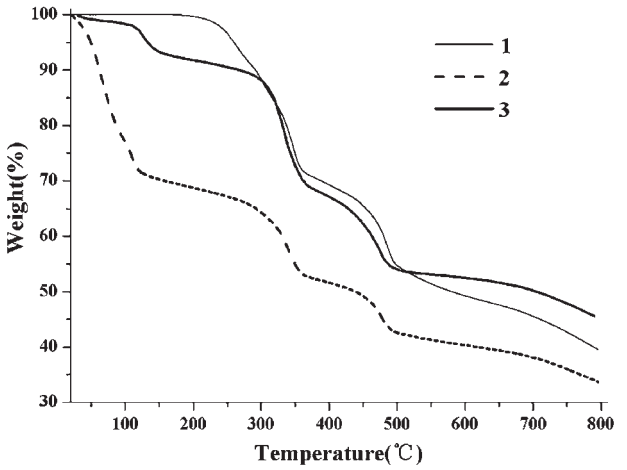

Figure 5. TGA of complex **1**−**3**: thin line for **1**; dotted thick line for **2**; thick line for **3**, respectively.

which are occupied by the lattice water molecules. About 32.6% solvent-accessible volume is calculated by PLATON program.

It is interesting to compare the bridging fashions of the btca ligand in **1**−**3** (Figure 4). We find that the ligand has a bidentate pyrazolate-like mode bridging two cupric ions and monodentate carboxyl group bridging another cupric ion resulting in the two-dimensional (2D) network of **1**. The bidentate imidazolate-like binding mode with the capability of bridging two cupric ions can be found in **2**. The deprotonated carboxylic group accepts hydrogen bonding from H_2btca and plays an indispensable role in the hydrogen-bonded nanotubular structure formation of **2**. Tridentate coordination mode of 1,2,3-triazolate group as well as monodentate forms of carboxyl group containing in one btca ligand lead to the 3D porous honeycomb-like structure of **3**. It is noteworthy that some special structures based on clusters, macrocycles, cages, and chains with metal ions as centers and btca as linkers in this paper are elucidated, which enrich molecular tectonics in the field of supramolecular coordination chemistry.

Thermal Stability. The TGA curve (Figure 5) displays that **1** is stable up to 200 °C and then decomposes upon further heating. The TGA curve of **2** shows an initial weight loss of 30.59% from room temperature to 177 °C, corresponding to the removal of five waters (calculated 30.58%) including all coordinated water molecules per formula unit, suggesting low stability of **2** after the release of water molecules. With regard to **3**, the first weight loss of 3.27% from room temperature to 125 °C corresponds to removal of a water molecule (calculated 3.26%), and then the 3D framework loses weight from 125 to 264 °C (observed 6.60%, calculated 6.56%) revealing evacuation of one coordinated water and half a HCl composed by half a hydrogen cation and half a chloride per formula unit. Then, the decomposition of the btca ligand, with the framework collapse, occurs upon heating subsequently. After **3** was outgased, with heating at 140 and 280 °C under vacuum, respectively, the PXRD patterns were similar to the simulated pattern of **3** (Figure 6), which suggests that the desolvated framework keeps its crystalline state.

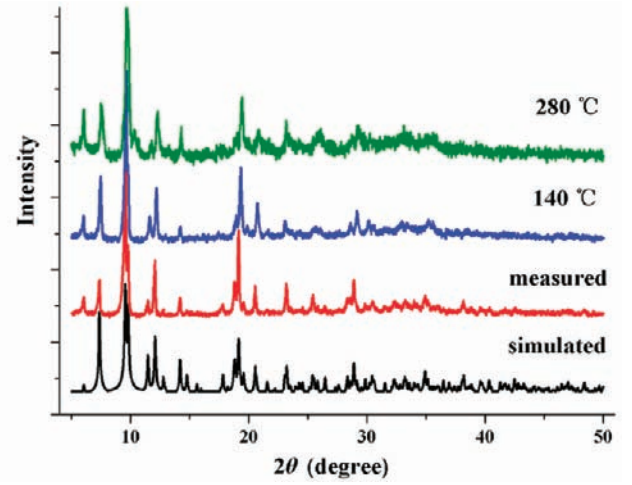

Figure 6. PXRD patterns of **3**: simulated (black), measured (red), desolvated by heating at 140 °C (blue), and at 280 °C (olive), respectively.

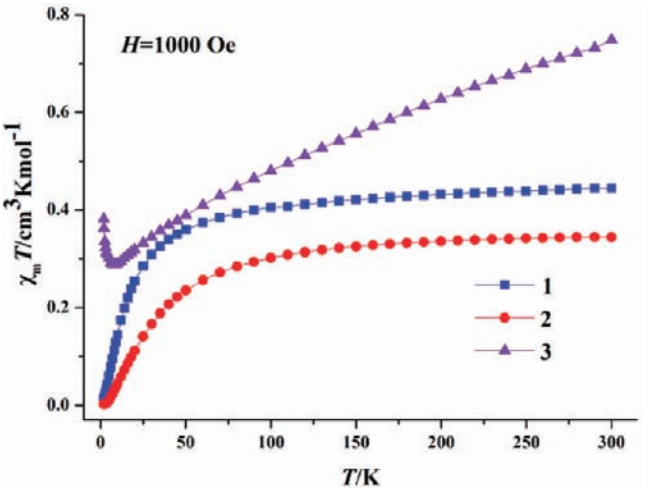

Figure 7. Temperature-dependent magnetic susceptibilities of **1**−**3** under a static field of 1000 Oe. The experimental data for **1**, **2**, and **3** is shown as blue squares, red circles, an violet triangles, respectively.

Magnetic Properties. Solid-state, variable-temperature (2−300 K) magnetic susceptibility measurements of the three compounds using an applied field of 1000 Oe are given in Figure 7. The $\chi_m T$ value of **1** is 0.445 cm^3 mol^{-1} K at 300 K, slightly larger than that expected for an uncoupled Cu(II) ion with g = 2.0 (0.375 cm^3 mol^{-1} K), thus supporting the presence of antiferromagnetic interactions between Cu(II) ions. The $\chi_m T$ curve exhibits a continuous decrease upon cooling down to a value very close to zero. For **2**, The $\chi_m T$ data shows a behavior characteristic of very

dx.doi.org/10.1021/ic201571n |*Inorg. Chem.* 2011, 50, 11032–11038

weak coupled Cu(II) systems, comparable to isolated mononuclear species containing such a metal center. This way, the magnetic susceptibility value at 300 K is 0.344 $cm^3\ mol^{-1}$ K, being slightly less than the spin-only value (0.375 $cm^3\ mol^{-1}$ K) of one isolated Cu(II) ion. Between 25 and 300 K for **1**, 80 and 300 K for **2**, the χ^{-1} versus T curves can be well fit by the Curie−Weiss law, leading to the following parameters: for **1**, C = 0.466 $cm^3\ mol^{-1}$ K, θ = −33.137 K; for **2**, C = 0.374 $cm^3\ mol^{-1}$ K, θ = −62.482 K (Figure S5 and S6). The negative θ values indicate antiferromagnetic coupling dominating these systems. However, the $\chi_m T$ value of **3** is 0.75 $cm^3\ mol^{-1}$ K at 300 K, which is appreciably lower than the theoretical value of 0.936 $cm^3\ mol^{-1}$ K for two and a half uncoupled $S = {}^1/_2$ spins. There is not a plateau at room temperature owing to the presence of both intra- and intercluster antiferromagnetic coupling. It is noteworthy that the $\chi_m T$ values of **3** continuously decrease upon cooling and reach to the minimum value (0.289 $cm^3\ mol^{-1}$ K) at 8 K and then increase to 0.382 $cm^3\ mol^{-1}$ K at 2 K, which exhibits weak ferromagnetic behavior at low temperature for **3**. Between 140 and 290 K, the χ^{-1} versus T data can be well fit by the Curie−Weiss law with C = 1.00 $cm^3\ mol^{-1}$ K, θ = −135.056 K (Figure S7). The relatively big negative Weiss constant indicates a dominating intracluster antiferromagnetic coupling.

CONCLUSIONS

In summary, three coordination assemblies with different dimensional structures were synthesized using cupric metal ions and benzotriazole-5-carboxylate acid as the organic linker in different solvent media. This work demonstrates that the variation of reaction conditions is critical to successful syntheses of coordination polymers with distinct properties in some particular systems. The versatile coordination modes of btca ligands result in diverse structures wherein the bidentate pyrazole-like mode of btca contributes to a 2D layer structure with (4.8^2) topology of **1**, and the bidentate imidazole-like mode focuses on rare octagonal metallomacrocyles which link together to be a hydrogen-bonded nanotubular structure of **2**. However, the 1,2,3-triazole coordination mode leads to the most complicated 3D microporous framework with honeycomb channels in **3**. Simultaneously, the discrete octagon in **2**, pentacluster, cage-like hexanuclear cluster, and strip-shaped chain in **3** are rare in benzotriazole-5-carboxylate system. The solvent molecules of water (**1**, **2**, **3**) and chlorine hydride (**3**) can affect the thermal properties via intermolecular interactions with the host frameworks. Finally, the magnetic properties of **1**−**3** indicate the antiferromagnetic behavior of **1** and **2** and weak ferromagnetic behavior at low temperature of **3**. We are currently exploring the effect of planarization in larger nanorings, and the system will be applied to other metal ion cases with more interesting properties in our future work.

ASSOCIATED CONTENT

Supporting Information. X-ray crystallographic data in CIF format, coordination environment of three Cu^{2+} ions in **3**, and PXRD patterns and detailed magnetic analyses of **1**−**3**. This material is available free of charge via the Internet at http://pubs.acs.org.

AUTHOR INFORMATION

Corresponding Author

*E-mail: xchuang@stu.edu.cn. Fax: +86 754 8290-2589.

ACKNOWLEDGMENT

This work was supported by MOE of China (NCET09-0089), NSFC (20801034 and 21171113), and NSF of Guangdong Province (8251503101000001 and 06027203).

REFERENCES

(1) (a) An, J.; Rosi, N. L. *J. Am. Chem. Soc.* **2010**, *132*, 5578. (b) Han, S.-B.; Wei, Y.-H.; Valente, C.; Lagzi, I.; Gassensmith, J. J.; Coskun, A.; Stoddart, J. F.; Grzybowski, B. A. *J. Am. Chem. Soc.* **2010**, *132*, 16358. (c) Kuppler, R. J.; Timmons, D. J.; Fang, Q.-R.; Li, J.-R.; Makal, T. A.; Young, M. D.; Yuan, D.-Q.; Zhao, D.; Zhuang, W.-J.; Zhou, H.-C. *Coord. Chem. Rev.* **2009**, *253*, 3042.

(2) (a) Dong, Y.-B.; Zhang, Q.; Liu, L.-L.; Ma, J.-P.; Tang, B.; Huang, R.-Q. *J. Am. Chem. Soc.* **2007**, *129*, 1514. (b) Su, C.-Y.; Cai, Y.-P.; Chen, C.-L.; Smith, M. D.; Kaim, W.; Loye, H. C. *J. Am. Chem. Soc.* **2003**, *125*, 8595. (c) Chen, C.-L.; Tan, H.-Y.; Yao, J.-H.; Wan, Y.-Q.; Su, C.-Y. *Inorg. Chem.* **2005**, *44*, 8510. (d) Liu, Z.-M.; Liu, Y.; Zheng, S.-R.; Yu, Z.-Q.; Mei, P.; Su, C.-Y. *Inorg. Chem.* **2007**, *46*, 5814. (e) Huang, X.-C.; Zhang, J.-P.; Chen, X.-M. *J. Am. Chem. Soc.* **2004**, *126*, 13218.

(3) (a) Lin, J.-B.; Zhang, J.-P.; Zhang, W.-G.; Xue, W.; Xue, D.-X.; Chen, X.-M. *Inorg. Chem.* **2009**, *48*, 6652. (b) Wang, X.-L.; Hu, H.-L.; Tian, A.-X.; Lin, H.-Y.; Li, J. *Inorg. Chem.* **2010**, *49*, 10299. (c) Nakabayashi, K.; Ozaki, Y.; Kawano, M.; Fujita, M. *Angew. Chem., Int. Ed.* **2008**, *47*, 2046. (d) Zhang, J.-J.; Wojtas, L.; Larsen, R. W.; Eddaoudi, M.; Zaworotko, M. J. *J. Am. Chem. Soc.* **2009**, *131*, 17040. (e) Horike, S.; Shimomura, S.; Kitagawa, S. *Nat. Mater.* **2009**, *1*, 695. (f) Kawamichi, T.; Haneda, T.; Kawano, M.; Fujita, M. *Nature* **2009**, *461*, 633. (g) Zhang, J.; Chen, S.-M.; Nieto, R.-A.; Wu, T.; Feng, P.-Y.; Bu, X.-H. *Angew. Chem., Int. Ed.* **2010**, *49*, 1267. (h) Zhang, J.-P.; Huang, X.-C.; Chen, X.-M. *Chem. Soc. Rev.* **2009**, *38*, 2385. (i) Ma, L.-Q.; Abney, C.; Lin, W.-B. *Chem. Soc. Rev.* **2009**, *38*, 1248. (j) Li, J.-R.; Kuppler, R. J.; Zhou, H.-C. *Chem. Soc. Rev.* **2009**, *38*, 1477.

(4) (a) Zhang, J.-P.; Chen, X.-M. *Chem. Commun.* **2006**, *42*, 1684. (b) Wu, T.; Zhang, J.; Zhou, C.; Wang, L.; Bu, X.-H.; Feng, P.-Y. *J. Am. Chem. Soc.* **2009**, *131*, 6111. (c) Huang, X.-C.; Luo, W.; Shen, Y.-F.; Lin, X.-J.; Li, D. *Chem. Commun.* **2008**, *44*, 3995. (d) Wei, G.; Shen, Y.-F.; Li, Y.-R.; Huang, X.-C. *Inorg. Chem.* **2010**, *49*, 9191. (e) Shao, K.-Z.; Zhao, Y.-H.; Xing, Y.; Lan, Y.-Q.; Wang, X.-L.; Su, Z.-M.; Wang, R.-S. *Cryst. Growth Des.* **2008**, *8*, 2986. (f) Ouellette, W.; Prosvirin, A. V.; Whitenack, K.; Dunbar, K. R.; Zubieta, J. *Angew. Chem., Int. Ed.* **2009**, *48*, 2140. (g) Hao, H.-G.; Zheng, X.-D.; Lu, T.-B. *Angew. Chem., Int. Ed.* **2010**, *49*, 8148. (h) Lin, J.-B.; Zhang, J.-P.; Chen, X.-M. *J. Am. Chem. Soc.* **2010**, *132*, 6654.

(5) (a) Ma, L.; Jin, A.; Xie, Z.-G.; Lin, W.-B. *Angew. Chem., Int. Ed.* **2009**, *48*, 9905. (b) Li, J.-R.; Zhou, H.-C. *Nature Chem.* **2010**, *2*, 893. (c) Cheng, X.-N.; Xue, W.; Chen, X.-M. *Eur. J. Inorg. Chem.* **2010**, 3850. (d) Luo, J.-H.; Xu, H.-W.; Liu, Y.; Zhao, Y.-S.; Daemen, L. L.; Brown, C.; Timofeeva, T. V.; Ma, S.-Q.; Zhou, H.-C. *J. Am. Chem. Soc.* **2008**, *130*, 9626. (e) Ma, S.-Q.; Simmons, J. M.; Sun, D.-F.; Yuan, D.-Q.; Zhou, H.-C. *Inorg. Chem.* **2009**, *48*, 5263. (f) Ma, S.-Q.; Sun, D.-F.; Yuan, D.-Q.; Wang, X.-S.; Zhou, H.-C. *J. Am. Chem. Soc.* **2009**, *131*, 6445. (g) Zhao, D.; Yuan, D.-Q.; Sun, D.-F.; Zhou, H.-C. *J. Am. Chem. Soc.* **2009**, *131*, 9186. (h) Zhuang, W.-J.; Ma, S.-Q.; Wang, X.-S.; Yuan, D.-Q.; Li, J.-R.; Zhao, D.; Zhou, H.-C. *Chem. Commun.* **2010**, *46*, 5223. (i) Ma, S.-Q.; Simmons, J. M.; Yuan, D.-Q.; Li, J.-R.; Weng, W.; Liu, D.-J.; Zhou, H.-C. *Chem. Commun.* **2009**, *45*, 4049. (j) Ma, L.-l.; Lin, W.-B. *Angew. Chem., Int. Ed.* **2009**, *48*, 3637.

(6) (a) Yamauchi, Y.; Yoshizawa, M.; Fujita, M. *J. Am. Chem. Soc.* **2008**, *130*, 5832. (b) Yamauchi, Y.; Yoshizawa, M.; Akita, M.; Fujita, M. *J. Am. Chem. Soc.* **2010**, *132*, 960. (c) Murase, T.; Otsuka, K.; Fujita, M. *J. Am. Chem. Soc.* **2010**, *132*, 7864. (d) Osuga, T.; Murase, T.; Ono, K.; Yamauchi, Y.; Fujita, M. *J. Am. Chem. Soc.* **2010**, *132*, 15553. (e) Murase, T.; Fujita, M. *Chem. Rec.* **2010**, *10*, 342.

(7) (a) Alkordi, M.-H.; Brant, J.-A.; Wojtas, L.; Kravtsov, V.-C.; Cairns, A.-J.; Eddaoudi, M. *J. Am. Chem. Soc.* **2009**, *131*, 17753. (b) Lu, W.-G.; Su, C.-Y.; Lu, T.-B.; Jiang, L.; Chen, J.-M. *J. Am. Chem. Soc.* **2006**,

128, 34. (c) Gu, J.-Z.; Lu, W.-G.; Jiang, L.; Zhou, H.-C.; Lu, T.-B. *Inorg. Chem.* **2007**, *46*, 5835. (d) Lu, W.-G.; Jiang, L.; Feng, X.-L.; Lu, T.-B. *Inorg. Chem.* **2009**, *48*, 6997. (e) Lu, W.-G.; Jiang, L.; Lu, T.-B. *Cryst. Growth Des.* **2010**, *10*, 4310. (f) Nouar, F.; Eckert, J.; F. Eubank, J.; Forster, P.; Eddaoudi, M. *J. Am. Chem. Soc.* **2009**, *131*, 2864. (g) Sava, D. F.; Kravtsov, V. Ch.; Eckert, J.; Eubank, J. F.; Nouar, F.; Eddaoudi, M. *J. Am. Chem. Soc.* **2009**, *131*, 10394.

(8) (a) Yue, Y.-F.; Wang, B.-W.; Gao, E.-Q.; Fang, C.-J.; He, C.; Yan, C.-H. *Chem. Commun.* **2007**, *43*, 2034. (b) Zhang, W.-X.; Xue, W.; Zheng, Y.-Z.; Chen, X.-M. *Chem. Commun.* **2009**, *45*, 3804. (c) Yuan, G.; Shao, K.-Z.; Wang, X.-L.; Lan, Y.-Q.; Du, D.-Y.; Su, Z.-M. *CrystEngComm* **2010**, *12*, 1147. (d) Zhang, W.-X.; Xue, W.; Lin, J.-B.; Zheng, Y.-Z.; Chen, X.-M. *CrystEngComm* **2008**, *10*, 1770. (e) Yuan, G.; Shao, K.-Z.; Du, D.-Y.; Wang, X.-L.; Su, Z.-M. *Sci. China: Chem.* **2010**, *53*, 2177.

(9) (a) Liu, Z.; Chen, Y.; Liu, P.; Wang, J.; Huang, M.-H. *J. Solid State Chem.* **2005**, *178*, 2306. (b) Guo, Z.-G.; Yuan, D.-Q.; Bi, W.-H.; Li, X.-J.; Wang, Y.-Q.; Cao, R. *J. Mol. Struct.* **2006**, *178*, 106. (c) Guo, Z.-G.; Li, X.-J.; Gao, S.-Y.; Li, Y.-F.; Cao, R. *J. Mol. Struct.* **2007**, *846*, 123. (d) Deng, Q.-J.; Zeng, M.-H.; Liang, H.; Ng, W. S.; Huang, K.-L. *Acta Crystallogr., Sect. E* **2010**, *62*, m1293.

(10) (a) Yao, Y.-L.; Che, Y.-X.; Zheng, J.-M. *Cryst. Growth Des.* **2008**, *8*, 2299. (b) Wei, Y.-Q.; Yu, Y.-F.; Wu, K.-C. *Cryst. Growth Des.* **2008**, *8*, 2087. (c) Li, Z.-Y.; Dai, J.-W.; Wang, N.; Qiu, H.-H.; Yue, S.-T.; Liu, Y.-L. *Cryst. Growth Des.* **2010**, *10*, 2746. (d) Liu, Y.-R.; Li, L.; Yang, T.; Yu, X.-W.; Su, C.-Y. *CrystEngComm* **2009**, *11*, 2712. (e) Wang, Z.-X.; Wu, Q.-F.; Liu, H.-J.; Shao, M.; Xiao, H.-P.; Li, M.-X. *CrystEngComm* **2010**, *12*, 1139. (f) Wei, Y.-Q.; Yu, Y.-F.; Sa, R.-J.; Li, Q.-H.; Wu, K.-C. *CrystEngComm* **2009**, *11*, 1054.

(11) (a) Gurunatha, K. L.; Uemura, K.; Maji, T. K. *Inorg. Chem.* **2008**, *47*, 6578. (b) Peng, G.; Qiu, Y.-C.; Liu, Z.-H.; Liu, B.; Deng, H. *Cryst. Growth Des.* **2010**, *10*, 114. (c) Guo, Z.-G.; Cao, R.; Li, X.-J.; Yuan, D.-Q.; Bi, W.-H.; Zhu, X.-D.; Li, Y.-F. *Eur. J. Inorg. Chem.* **2007**, 742.

(12) (a) Morris, W.; Leung, B.; Furukawa, H.; Yaghi, O. K.; He, N.; Hayashi, H.; Houndonougbo, Y.; Asta, M.; Laird, B. B.; Yaghi, O. M. *J. Am. Chem. Soc.* **2010**, *132*, 11006. (b) Banerjee, R.; Furukawa, H.; Britt, D.; Knobler, C.; O'Keeffe, M.; Yaghi, O. M. *J. Am. Chem. Soc.* **2009**, *131*, 3875. (c) Banerjee, R.; Phan, A.; Wang, B.; Knobler, C.; Furukawa, H.; O'Keeffe, M.; Yaghi, O. M. *Science* **2008**, *319*, 939. (d) Furukawa, H.; Ko, N.; Go, Y. B.; Aratani, N.; Choi, S. B.; Choi, E.; Yazaydin, Ö.; Q. Snurr, R.; O'Keeffe, M.; Kim, J.; Yaghi, O. M. *Science* **2010**, *239*, 424.

(13) (a) Zhang, X.-M.; Hao, Z.-M.; Zhang, W.-X.; Chen, X.-M. *Angew. Chem., Int. Ed.* **2007**, *46*, 3456. (b) Uhl, W.; Vo, M.; Layh, M.; Rogel, F. *Dalton Trans.* **2010**, *39*, 3160. (c) Lu, R.-Y.; Luan, G.-Y.; Han, Z.-B. *Acta Crystallogr., Sect. C* **2010**, *66*, m283. (d) Lu, R.-Y.; Han, Z.-B. *Russ. J. Coord. Chem.* **2011**, *37*, 172.

(14) (a) Zhao, J.-A.; Mi, L.-W.; Hu, J.-Y.; Hou, H.-W.; Fan, Y.-T. *J. Am. Chem. Soc.* **2008**, *130*, 15222. (b) Ene, C. D.; Madalan, A. M.; Maxim, C.; Jurca, B.; Avarvari, N.; Andruh, M. *J. Am. Chem. Soc.* **2009**, *131*, 4586. (c) Bai, Y.-L.; Tangoulis, V.; Huang, R.-B.; Zheng, L.-S.; Tao, J. *Chem.—Eur. J.* **2009**, *15*, 2377. (d) Frischmann, P. D.; Guieu, S.; Tabeshi, R.; MacLachlan, M. J. *J. Am. Chem. Soc.* **2010**, *132*, 7668.

(15) (a) Wu, T.; Bu, X.-H.; Zhang, J.; Feng, P.-Y. *Chem. Mater.* **2008**, *20*, 7377. (b) Li, G.; Yu, W.-B.; Cui, Y. *J. Am. Chem. Soc.* **2008**, *130*, 4582. (c) Huang, X.-C.; Zhang, J.-P.; Chen, X.-M. *J. Am. Chem. Soc.* **2004**, *126*, 13218.